

Dual-wavelength photoacoustic imaging of a photoswitchable reporter protein

Hakan Dortay^a, Julia Märk^a, Asja Wagener^d, Edward Zhang^e, Carsten Grötzinger^d,
Peter Hildebrandt^b, Thomas Friedrich^b, Jan Laufer^{a,c,*}

^aInstitut für Optik und Atomare Physik, ^bInstitut für Chemie, Technische Universität Berlin,
Straße des 17. Juni 135, 10623 Berlin, Germany

^cInstitut für Radiologie, ^dMolekulares Krebsforschungszentrum,

Charité – Universitätsmedizin Berlin, Charitéplatz 1, 10117 Berlin, Germany

^eDepartment of Medical Physics and Bioengineering, University College London, Gower Street,
London WC1E 6BT, UK

ABSTRACT

Photoacoustic (PA) imaging has been shown to provide detailed 3-D images of genetically expressed reporters, such as fluorescent proteins and tyrosinase-induced melanin. Their unambiguous detection *in vivo* is a vital prerequisite for molecular imaging of biological processes at a cellular and molecular level. This typically requires multiwavelength imaging and spectral unmixing techniques, which can be computationally expensive. In addition, fluorescent proteins often exhibit fluence-dependent ground state depopulation and photobleaching which can adversely affect the specificity of unmixing methods. To overcome these problems, a phytochrome-based reporter protein and a dual-wavelength excitation method have been developed to obtain reporter-specific PA contrast. Phytochromes are non-fluorescent proteins that exhibit two isomeric states with different absorption spectra. Using dual-wavelength excitation pulses in the red and near-infrared wavelength region, these states can be switched, resulting in a modulation of the total absorption coefficient, and hence the PA signal amplitude. Since this is not observed in endogenous chromophores, signals acquired using simultaneous pulses can be subtracted from the sum of signals obtained from separate pulses to provide a reporter-specific contrast mechanism and elimination of the tissue background. PA signals measured in protein solutions using separate and simultaneous excitation pulses at 670 nm and 755 nm ($< 6 \text{ mJ cm}^{-2}$) showed a difference in amplitude of a factor of five. Photobleaching was not observed. To demonstrate suitability for *in vivo* applications, mammalian cells were transduced virally to express phytochrome, and imaged in tissue phantoms and in mice in an initial preclinical study. The results show that this method has the potential to enable deep-tissue PA reporter gene imaging with high specificity.

Keywords: reporter genes, photoswitchable proteins, dual-wavelength imaging, phytochromes

*jan.laufer@tu-berlin.de

1. INTRODUCTION

The feasibility of *in vivo* PA imaging of genetically expressed reporters has already been demonstrated in a number of studies. Reported approaches included the genetic expression of the enzyme tyrosinase, which resulted in the synthesis of the highly photostable pigment eumelanin¹⁻³. Tyrosinase-based expression of eumelanin has been shown to combine photostable optical properties and an inherent amplification of pigment concentration, and hence strong PA contrast, due to the enzymatic conversion of tyrosine to melanin. Other studies focused on the development and application of existing fluorescent reporter proteins and chromoproteins⁴⁻⁶. However, fluorescent proteins have been shown to result in reduced PA signal amplitudes due to ground state depopulation and fluorescence emission⁶ and the absorption maxima of most fluorescent proteins coincides with high attenuation in blood, which is disadvantageous for deep tissue imaging applications. More importantly, most fluorescent proteins photobleach when exposed to the ns excitation pulses typically

used in PA imaging even when the fluence is significantly lower than the maximum permissible exposure⁶. This alone makes the detection of fluorescent reporter proteins challenging. However, this is compounded by lack of generally applicable and experimentally validated methods for molecular PA tomography. Typical approaches involve the acquisition of multiwavelength images and the application of some form of spectral unmixing, such as model-based inversion schemes. While the considerable computational burden is a significant drawback, it is the reliance on accurate *a priori* information, such as the wavelength dependence of the absorption coefficient, which precludes the detection of fluorescent proteins using this approach. The detection of photostable absorbers, such as eumelanin, is also not trivial since generally applicable methods for the recovery of unambiguous chromophore distributions from *in vivo* 3-D tomography images are not available. There is a clear need for novel genetic reporters and new methods for their detection. Phytochromes, which are light sensitive proteins that originate from plants and bacteria, provide a unique combination of advantageous properties, such as absorption in the red to near-infrared wavelength region, photostability, and - most importantly - photoswitchable absorption. In this paper, the methods for the expression of a phytochrome-based photoswitchable reporter protein in mammalian cells and its detection in 3-D tomographic images acquired *in vivo* in a small animal tumour model are described.

2. BACKGROUND

2.1 PA signal generation in phytochromes

Phytochromes, such as AGP1 (*from Agrobacterium tumefaciens*)⁷⁻⁹, contain the light-absorbing pigment biliverdin, which is covalently bound to the protein barrel, and exhibit two isomeric states, Pr and Pfr, with distinct absorption spectra as shown in Figure 1. Pr and Pfr states can be switched depending on the wavelength of the illumination. For example, illumination using light in the red wavelength region (650 nm to 690 nm) will cause the phytochromes to induce a Pr → Pfr switch while illumination using near-infrared (NIR) light (730 nm to 780 nm) will cause Pfr → Pr transition. A PA difference signal is obtained by subtracting the sum of PA waveforms acquired using excitation pulses in the red and the near-infrared wavelength region separately from the waveform acquired using simultaneous the red and near-infrared wavelength regions. The difference signal amplitude is non-zero for phytochromes and zero for endogenous tissue chromophores, such as blood, lipids, and water. The optically induced change in the wavelength dependence of absorption can therefore be exploited for detection in PA tomography images as it provides a unique and unambiguous contrast mechanism.

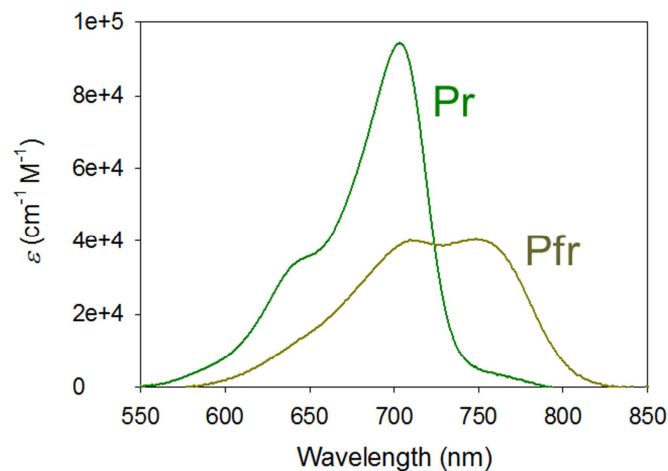


Figure 1. Spectra of the specific extinction coefficient of the isomeric states Pr and Pfr exhibited by phytochrome AGP1.

3. MATERIALS AND METHODS

In section 3.1, the methods for the expression of phytochrome AGP1 in bacteria and human cell lines are described. Section 3.2 describes the *in vitro* characterization of purified solutions of AGP1 using PA spectroscopy, section 3.3 presents the methods developed for *in vivo* imaging of AGP1 expressing tumour cells.

3.1 Phytochrome expression in bacteria and mammalian cells

Plasmids encoding either phytochrome AGP1 or the near-infrared fluorescent protein iRFP were created based on a genetic sequence that was optimised for mammalian expression and introduced into *Escherichia Coli* bacteria for protein production. The bacterial cells were lysed, centrifuged, and filtered to obtain solutions of purified AGP1 in phosphate-buffered saline (PBS) solution for *in vitro* measurements in cuvettes using PA spectroscopy (section 3.2).

In order to transduce mammalian cells, lentivirus containing the gene encoding AGP1 and the fluorescent protein mCherry were produced in HEK cells. The virus was then used to transduce human colorectal cancer cell line (HT29) in order to induce the stable co-expression of AGP1 and mCherry. The fluorescence of the latter was used to verify the success of the transduction and to obtain the highest expressing cells via FACS. The sorted cells were grown until sufficient cells were available for *in vivo* experiments.

3.2 *In vitro* characterisation of phytochrome AGP1

The experimental setup for the characterisation of purified AGP1 solutions is shown in Figure 2. A cuvette containing the protein solution was placed in a water bath and illuminated by the signal and idler outputs of an OPO laser system (PRO-270-50 and premiScan OPO, Newport Spectra-Physics). The output was controlled using shutters and neutral density filters and coupled into a 1.5 mm dia. fused silica fibre to homogenise the beam at the cuvette. The generated PA waves were detected using a large area piezoelectric transducer (Precision Acoustics Ltd). PA difference signals were measured as a function of the excitation wavelength to determine the optimum combination of the signal and idler wavelengths in the red and NIR region. In addition, photobleaching was investigated by recording the PA signal amplitude as a function of the number of excitation pulses in solutions of AGP1 and iFRP using simultaneous signal and idler illumination.

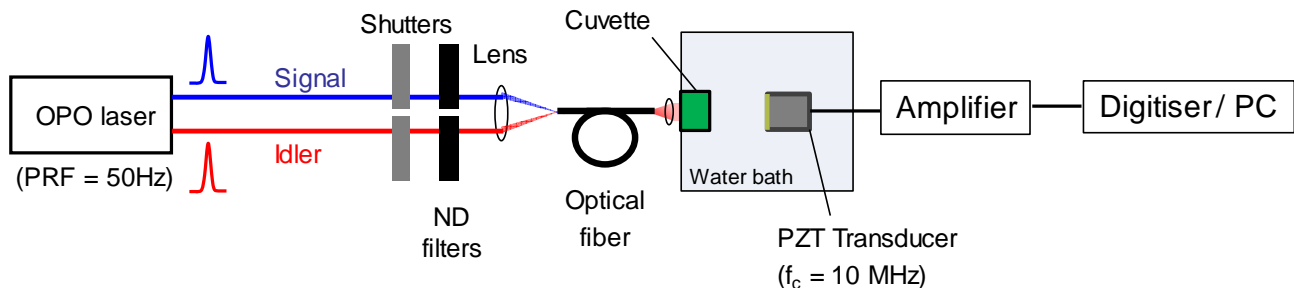


Figure 2. Experimental setup for the *in vitro* characterisation of purified AGP1 solutions.

3.3 PA imaging of tissue phantoms

To demonstrate the detection of AGP1 using difference imaging, 2-D cross sectional images of a tissue phantom were acquired using a PA scanner based on a Fabry-Pérot polymer film ultrasound sensor¹¹. The phantom consisted of polymer tubes (600 μm inner dia), which were filled with either a copper chloride solution to represent endogenous tissue chromophores, such as haemoglobin, or purified AGP1 solution. The tubes were suspended in a scattering lipid suspension with a reduced scattering coefficient of approximately 1 mm^{-1} . PA waveforms were generated in backward mode using excitation pulses at 670 nm and 755 nm. From the recorded waveforms, 2-D images were reconstructed using an FFT-based image reconstruction algorithm¹² for the subsequent calculation of a difference image.

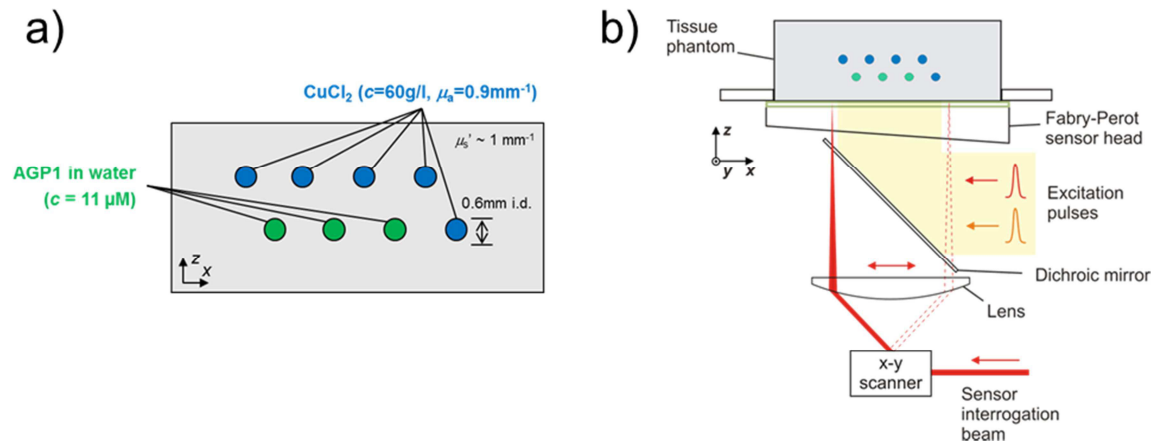


Figure 3. Experimental setup for PA difference imaging of tissue phantoms. 2-D cross sectional images were obtained using a PA scanner based on a Fabry-Pérot polymer film ultrasound sensor.

3.4 *In vivo* PA imaging of AGP1

5×10^6 AGP1-expressing HT29 cells in PBS were inoculated into nude mice subcutaneously. The animals were anaesthetised using isoflurane and 3-D image data sets were acquired at four time points over a period of 28 days. In order to minimise motion artefacts during the raster scan based readout of the sensor, the image acquisition protocol was modified for *in vivo* measurements. To exploit the comparatively slow photoswitching time-course of AGP1 difference signals were acquired at each readout position of the sensor by switching excitation at 670 nm on and off whilst keeping excitation at 755 nm constant. This modulated the Pr – Pfr photoequilibrium. PA signals were acquired in each illumination phase over a number of excitation pulses. Endogenous chromophores do not show slow changes in absorption, i.e. the change in PA signal amplitude as a result of switching 670 nm excitation is instantaneous and the signal amplitude remains constant during each illumination phase. By contrast, the relatively slow photoswitching of AGP1 results in a gradual, asymptotic change in PA signal amplitude following a switch in 670 nm excitation. By calculating the difference between the PA signal amplitude of the first and subsequent waveforms within an illumination phase, PA difference signals were obtained at each sensor readout position in which the amplitude is greater than zero for AGP1 and zero for all other tissue chromophores.

4. RESULTS

4.1 PA cuvette measurement in purified solutions of phytochrome AGP1

In vitro PA cuvette measurements in purified AGP1 solutions showed that the combination of excitation wavelengths at which the PA difference signal is at a maximum are 670 nm and 755 nm when a single OPO laser system is used. By varying the relative fluence of signal and idler beams whilst maintaining a constant total fluence, it was shown that the difference signal is at a maximum for 30% signal fluence and 70% idler fluence at the optimum wavelengths. This is explained by the relative efficiencies of the AGP1 photoconversion from the Pr to the Pfr state and back (low quantum yield)⁷.

The results of the photobleaching experiments are shown in Figure 4. AGP1 produced a constant PA signal amplitude as a function of the number of excitation pulses while that measured in the near-infrared fluorescent protein iRFP shows a gradual decline, which is evidence of irreversible photobleaching¹³.

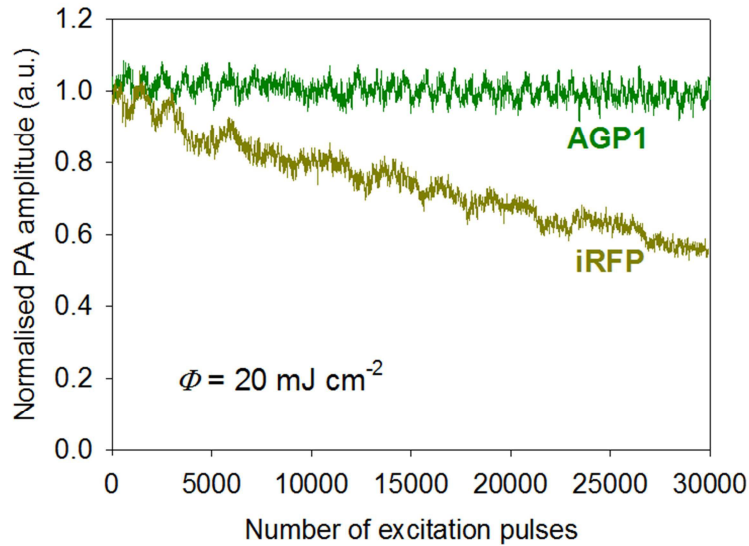


Figure 4. PA signal amplitude as a function of the number of excitation pulses measured in purified solutions of AGP1 and iRFP, showing evidence of photobleaching of iRFP. The excitation wavelengths were 670 nm and 755 nm.

4.2 PA difference imaging of tissue phantoms

Figure 5 shows 2-D cross sectional images of the tissue phantom. Figure 5(a) shows the sum of images acquired separately using excitation at 670 nm and 755 nm and Figure 5(b) shows the image acquired using simultaneous signal and idler excitation pulses. In both images the location of all tubes can be seen with very little visible difference between Figure 5(a) and (b). Figure 5(c) was obtained by subtracting Figure 5(a) from Figure 5(b) and shows the location of the tubes filled with AGP1 solution, thus demonstrating the principle of PA difference imaging of phytochrome-based reporter proteins. Due to the elimination of the background contrast, this method effectively provides detection of AGP1 that is limited only by the noise floor of the PA scanner. From the images shown in Figure 5, the noise equivalent concentration was estimated as 4 μM .

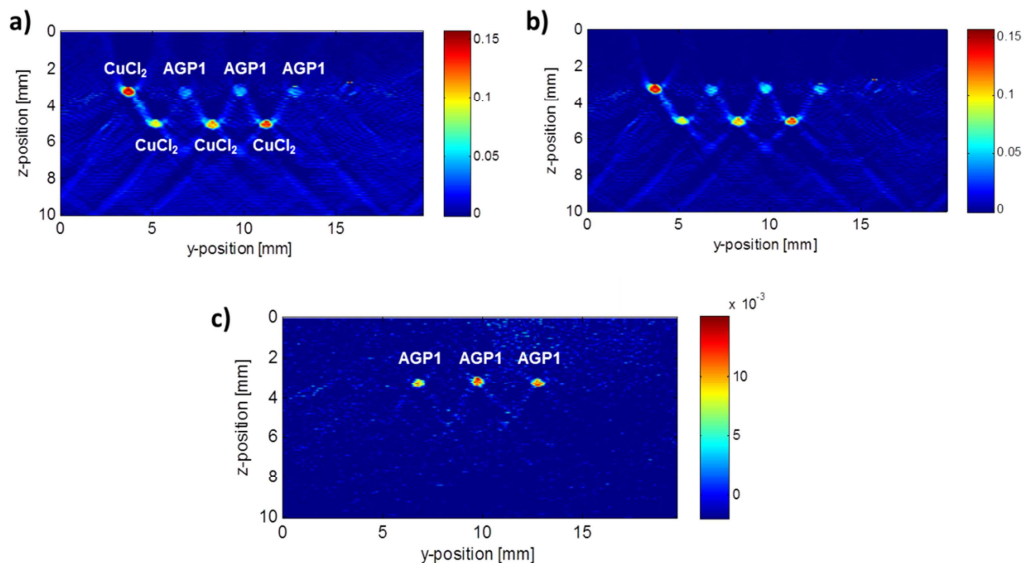


Figure 5. PA difference imaging of AGP1 in tissue phantoms. (a) Summed image of 2-D cross sectional PA images acquired using separate excitation at 670 nm and 755 nm, (b) PA image acquired using simultaneous excitation at 670 nm and 755 nm, and (c) the difference image obtained by subtracting (a) from (b).

4.3 PA imaging of AGP1 *in vivo*

Figure 6 shows maximum intensity projections (MIP) of *in vivo* 3-D image data sets of a subcutaneous tumour of AGP1-expressing HT29 cells. Figure 6(a) shows the morphological image, which was acquired at an excitation wavelength of 670 nm using conventional PA imaging. The dashed line marks the location of the tumour. Figure 6(b) shows the MIP of the data set that was acquired by exploiting the photoswitching time-course of AGP1 as described in section 3.4. The bright regions in the image show the location of the phytochrome reporter protein.

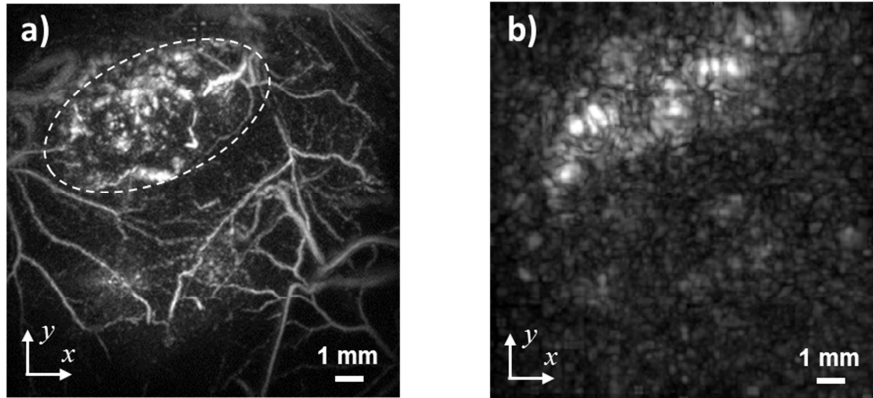


Figure 6. *x-y* MIPs of 3-D image data sets of subcutaneous AGP1-expressing human colorectal tumour cells (HT29). (a) MIP acquired using single wavelength excitation ($\lambda = 670$ nm) showing the vascular morphology of the tumour and the surrounding tissue. The dashed line shows the approximate location of the tumour. (b) MIP of image data set acquired using a method that exploits the photoswitching time-course of AGP1. The bright regions in the image indicate the location of AGP1, which agrees well with the corresponding location of the tumour shown in (a).

Importantly, this image acquisition protocol enabled not only the elimination of the background contrast produced by endogenous chromophores, such as blood, lipids, and water, but also the suppression of motion artefacts.

5. DISCUSSION

The cuvette measurements have shown that the excitation wavelengths and fluences can be optimised to obtain maximum difference signal amplitude. Given that the signal and idler wavelengths provided by a single OPO laser system are not independently tuneable, we believe that there is scope for further improvements if independent tuneable laser sources are used. In addition, it was shown that AGP1 did not show any evidence of photobleaching for fluences equivalent to the maximum permissible exposure. By contrast, the near-infrared fluorescent protein iRFP showed signs of irreversible photobleaching, which severely limits its application as a reporter protein for PA imaging.

While simple difference imaging was shown to enable the detection of AGP1 in tissue phantoms, this approach could not be applied to *in vivo* imaging. This was due to the raster scan-based waveform acquisition of the Farby-Pérot polymer film sensor, which results in image acquisition times of up to several minutes. Any movement in the imaged object gives rise to artefacts in the difference image, which typically show the vasculature. The image intensity of the artefacts can be significantly larger than that produced by the comparatively weak PA waves emitted by reporter proteins. In this study, this limitation was overcome by exploiting the slow change in optical absorption following photoswitching that is exhibited by phytochromes. Using a dual-wavelength photoswitching time-course imaging method, the unambiguous detection of AGP1 against the overwhelming image contrast produced by endogenous tissue chromophores and the confounding effects of tissue motion was demonstrated.

6. CONCLUSIONS

In this study, the *in vivo* PA detection and imaging of a phytochrome-based reporter protein is demonstrated. It has been shown that phytochrome AGP1 is expressed efficiently in mammalian cells following lentiviral transduction protocol, which has the potential to allow the transduction of a wide range of cell lines, including stem cells. Using an imaging

method based on dual-wavelength excitation and the detection of the photoswitching time-course, the phytochrome-based reporter AGP1 was detected in *in vivo* 3-D PA images against the overwhelming contrast of the endogenous tissue chromophores and the presence of tissue motion. Phytochromes combine a number of highly advantageous properties: 1) absorption in the near-infrared wavelength region, which is essential for deep tissue imaging, 2) photostable optical properties, 3) reversibly photoswitchable optical absorption, which provides an unambiguous PA contrast mechanism, and 4) expression in mammalian cells, which suggests a high degree of biocompatibility.

ACKNOWLEDGEMENTS

This work was funded by ERC Starting Grant 281356.

REFERENCES

- [1] Jathoul, A. P., Laufer, J., Ogunlade, O., Treeby, B., Cox, B., Zhang, E., Johnson, P., Pizzey, A. R., Philip, B., et al., "Deep *in vivo* photoacoustic imaging of mammalian tissues using a tyrosinase-based genetic reporter," *Nat. Photonics*(March), 1–8 (2015).
- [2] Laufer, J., Jathoul, A., Johnson, P., Zhang, E., Lythgoe, M., Pedley, R. B., Pule, M., Beard, P., "In vivo photoacoustic imaging of tyrosinase expressing tumours in mice," *Proc. SPIE, Photons Plus Ultrasound Imaging Sens.* **8223**, A. A. Oraevsky and L. V. Wang, Eds., 82230M – 82230M – 5 (2012).
- [3] Paproski, R. J., Forbrich, A. E., Wachowicz, K., Hitt, M. M., Zemp, R. J., "Tyrosinase as a dual reporter gene for both photoacoustic and magnetic resonance imaging.," *Biomed. Opt. Express* **2**(4), 771–780 (2011).
- [4] Razansky, D., Distel, M., Vinegoni, C., Ma, R., Perrimon, N., Köster, R. W., Ntziachristos, V., "Multispectral opto-acoustic tomography of deep-seated fluorescent proteins *in vivo*," *Nat. Photonics* **3**(7), 412–417 (2009).
- [5] Krumholz, A., Shcherbakova, D. M., Xia, J., Wang, L. V., Verkhusha, V. V., "Multicontrast photoacoustic *in vivo* imaging using near-infrared fluorescent proteins.," *Sci. Rep.* **4**, 3939 (2014).
- [6] Laufer, J., Jathoul, A., Pule, M., Beard, P., "In vitro characterization of genetically expressed absorbing proteins using photoacoustic spectroscopy," *Biomed. Opt. Express* **4**(11), 2477 (2013).
- [7] Lamparter, T., Michael, N., Mittmann, F., Esteban, B., "Phytochrome from *Agrobacterium tumefaciens* has unusual spectral properties and reveals an N-terminal chromophore attachment site.," *Proc. Natl. Acad. Sci. U. S. A.* **99**, 11628–11633 (2002).
- [8] Schumann, C., Gross, R., Wolf, M. M. N., Diller, R., Michael, N., Lamparter, T., "Subpicosecond midinfrared spectroscopy of the Pfr reaction of phytochrome Agp1 from *Agrobacterium tumefaciens*," *Biophys. J.* **94**(April), 3189–3197 (2008).
- [9] Wagner, J. R., Zhang, J., von Stetten, D., Günther, M., Murgida, D. H., Mroginski, M. A., Walker, J. M., Forest, K. T., Hildebrandt, P., et al., "Mutational analysis of *Deinococcus radiodurans* bacteriophytochrome reveals key amino acids necessary for the photochromicity and proton exchange cycle of phytochromes.," *J. Biol. Chem.* **283**(18), 12212–12226 (2008).
- [10] Mroginski, M. A., Murgida, D. H., Von Stetten, D., Kneip, C., Mark, F., Hildebrandt, P., "Determination of the Chromophore Structures in the Photoinduced Reaction Cycle of Phytochrome," *J. Am. Chem. Soc.* **126**(51), 16734–16735 (2004).
- [11] Zhang, E., Laufer, J., Beard, P., "Backward-mode multiwavelength photoacoustic scanner using a planar Fabry-Perot polymer film ultrasound sensor for high-resolution three-dimensional imaging of biological tissues.," *Appl. Opt.* **47**(4), 561–577 (2008).
- [12] Köstli, K. P. K. P., Beard, P. C., "Two-dimensional photoacoustic imaging by use of Fourier-transform image reconstruction and a detector with an anisotropic response," *Appl. Opt.* **42**(10), 1899–1908 (2003).
- [13] Filonov, G. S., Piatkevich, K. D., Ting, L.-M., Zhang, J., Kim, K., Verkhusha, V. V., "Bright and stable near-infrared fluorescent protein for *in vivo* imaging.," *Nat. Biotechnol.* **29**(8), 757–761 (2011).